

# Using Frequency Dependent Electric Space Heating Loads to Manage Frequency Disturbances in Power Systems

A. Rautiainen, S. Repo and P. Järventausta

**Abstract**—In this paper the use of frequency dependent space heating loads to manage frequency disturbances in power systems is investigated. Setting values of space heater thermostats are made dependent of locally measured network frequency. Studies are carried out through time domain simulations. Studies imply that the use of frequency dependent loads in frequency disturbance management is an efficient tool for managing power unbalances. This kind of load control method's consequences and harm to the users of the space heaters can be negligible, but the significance of this controllable load to the power system can be very high. It is very important to coordinate the operation of frequency dependent load carefully with other control actions taking into account the cold load pick-up phenomenon related to the use of this type of load.

**Index Terms**—Contingency reserve, demand response, domestic consumer, frequency stability, space heating

## I. INTRODUCTION

Today's society in developed countries is extremely dependent on electricity and a high level of service reliability is expected. In recent years there have been many serious frequency instability related wide-area power system blackouts in Europe [1] [2] and U.S. [3], and their costs, both economical and social, are high. Also, it is widely expected that intermittent power production, for example wind power and solar power, will increase rapidly at a global level, which sets new challenges for the control of power systems. Frequency stability is an issue of balance between power production and consumption. One way to influence this balance is to regulate power demand and usually large industrial loads are used for this purpose, but domestic loads could also be a very potential option.

In this article, the use of domestic electric space heating load to manage frequency disturbances is explored in a form of simulations using MATLAB and PSCAD software. The paper is organized as follows. In chapter II, the operation of

frequency dependent space heating load is described. In chapter III, the power system model and a thermodynamic model of space heating loads are described. In chapter IV simulation cases and simulation results are presented. Conclusions and discussion is presented in chapter V.

## II. OPERATION OF FREQUENCY DEPENDENT SPACE HEATING LOAD

In this study, the dynamic demand control (DDC) method, presented in [4] and further explored in [5], is applied to electric space heating loads. In the method the temperature settings of an electric space heater thermostat is frequency dependent in accordance with local frequency measurement. Figure 1 illustrates the control method of the loads used in these studies. Fig. 1 a) depicts normal thermostat action. Heater is switched on whenever temperature falls under a certain level, and off-switching occurs when temperature rises high enough. Thereby temperature varies around desired temperature  $T_{des}$ , which is set by user of the load through a manual thermostat adjustment. Fig. 1 b) illustrates DDC method in a disturbance reserve appliance. The set point value of temperature is now a function of grid frequency. Load reacts only at frequencies under  $f_1$  and maximum temperature deviation from normal operation is set to  $\Delta T_{max}$ .

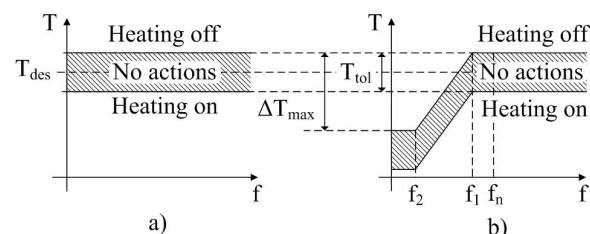


Fig. 1. a) Conventional thermostat action b) Control method of frequency dependent electric space heating load used in these studies (Figure is not in scale.)

## III. MODELING

In this chapter the models which are used in the simulations are introduced.

### A. Power system model

A 60 Hz and 230 kV power system illustrated in figure 2 was used in the simulations. The model was adopted from [6] p. 813–814 with little modifications. Parameters of the

The authors are grateful to the partners of the Eldig2\_VPP project “Active network management in electricity distribution” and INCA project “Interactive customer gateway” for the interesting real life research topic, comments, funding and research co-operation. The projects are financed by Tekes and several Finnish network companies, manufacturers and service companies.

All authors are with Department of Electrical Energy Engineering, Tampere University of Technology, P.O. Box 692, FI-33101 Tampere, Finland (e-mail: antti.rautiainen@tut.fi).

generators were adopted from [7]. All four generators included power system stabilizers that have the parameters presented in [6] p. 814. Turbine and speed governor models of the generators were adopted from [8]. Power lines in the middle of the figure (2 x 110 km) were originally (in [6]) twice as long as here. Shortening was made due to mitigate angle instability which appeared in the simulations. Angle stability was not under investigation in these studies. Ratings of generators were decreased to make the grid operate in very tight power conditions. Spinning reserve of generators was only about 40 MW.

Frequency dependent space heating loads were added as two similar aggregated groups  $L_7$  and  $L_8$  to the nodes 7 and 8 respectively in the power system. The total number of loads added was 580,000. Network's total load was ca. 2600 MW and the power (in normal conditions) of frequency dependent space heating load was ca. 260 MW (which is 10% of the total load) corresponding to 130 MW loads for each node 7 and 8. All loads in the system were modeled as constant impedance loads. In these studies space heating loads, which in reality are connected to the low voltage network, were scaled to transmission network voltage level and connected directly to the transmission network.

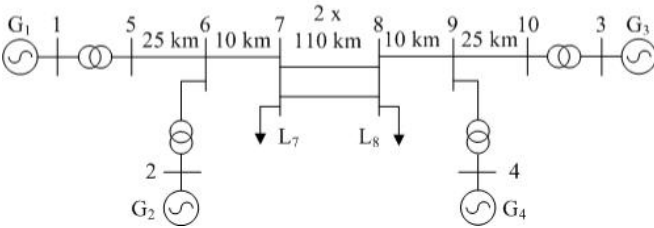


Fig. 2. Power system model used in the simulations

Frequencies which controlled the space heating loads  $L_7$  and  $L_8$  are measured at nodes 7 and 8, respectively. High frequency components of the frequency measurement signal are filtered off with a simple low-pass filter to avoid redundant operation of thermostat switches. Filter also includes a delay part, which simulates time delay between the time of occurrence of frequency disturbance in power system and the time of thermostat switch operation. Filter operates in accordance with a simple transfer function

$$H(s) = \frac{K}{1 - T_f s} e^{-sT_d} \quad (1)$$

where values of  $K$ ,  $T_f$  and  $T_d$  were 1.0, 0.2 s and 0.1 s respectively.

Frequency settings have a major impact on the operation of frequency dependent loads. In this work, frequency thresholds  $f_1$  (refer to fig. 1) of different loads were set at interval 59.7...59.9 Hz, and for each load frequency  $f_2$  were set 0.3 Hz lower than  $f_1$ .

### B. Thermodynamic modeling

To model the dynamic behavior of electric space heating load, a thermodynamic model describing the causality between in-door temperature and the heating power is needed.

In this work a very simple model, which is illustrated in fig. 3, is used. In the model the space which is heated (a room) is bounded with a control surface bounding a control volume. Control volume comprises all the mass which participates to heat storage and forms an effective heat capacity  $C$ , and homogeneous indoor temperature  $T_i$  is assumed in the control volume. Heat is brought into the system through heating equipment at rate  $P_{heat}$ . Heat is transferring outdoors through the system boundary at rate  $P_{loss}$ . Total thermal conductance  $G$  describes the thermal insulation level of the building, and  $T_o$  describes outdoor temperature.

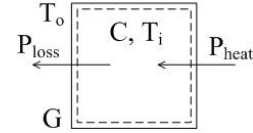


Fig. 3. Principle of the thermodynamic model of a space heating load

To get an equation that describes the indoor temperature with respect to time, an energy balance equation is first written for the system. Heat loss (heat which is conducting through the walls and windows) is directly proportional to total thermal conductance and to the difference between indoor and outdoor temperatures:

$$P_{loss} = G(T_i - T_o). \quad (2)$$

Indoor temperature change  $\Delta T_i$  within time interval  $\Delta t$  can be written as  $\Delta T_i = T_i(t + \Delta t) - T_i(t)$ .  $\Delta T_i$  corresponds to a change in the system's thermal energy  $C\Delta T_i$  which furthermore corresponds (according to the conservation of energy principle) to energy transferred by the difference between heating power  $P_{heat}$  and heat loss  $P_{loss}$ . Now we can write

$$C\Delta T_i = (P_{heat} - P_{loss})\Delta t. \quad (3)$$

Substituting (2) in to (3), dividing both sides of the equation by  $\Delta t$ , rearranging and letting the time interval approach zero ( $\Delta t \rightarrow 0$ ) we get a simple ordinary differential equation

$$C \frac{dT_i}{dt} + GT_i = P_{heat} + GT_o \quad (4)$$

which describes the temperature dynamics. If we treat  $C$ ,  $G$ ,  $P_{heat}$  and  $T_o$  as constants with respect to time, an analytical solution of the ordinary differential equation initial value problem, formed by (3) and the indoor temperature initial value  $T_i(0)$ , is

$$T_i(t) = \left( T_i(0) - \frac{P_{heat}}{G} - T_o \right) e^{-\frac{G}{C}t} + \frac{P_{heat}}{G} + T_o. \quad (5)$$

For numerical computing, it is necessary to determine parameters  $T_i(0)$ ,  $P_{heat}$ ,  $G$ ,  $T_o$  and  $C$ . Initial value of indoor temperature  $T_i(0)$  and outdoor temperature  $T_o$  are easy to determine, because their values can be chosen arbitrarily.

It is quite straightforward to approximate a typical value of thermal conductance  $G$ . In this work, the U-values of different structures which are needed in the determination process of  $G$ , are presented in table I. Thermal conductance is calculated as

$$G = \sum_{i=1}^n U_i A_i \quad (6)$$

where  $U_i$  is a U-value of structure  $i$ ,  $A_i$  is the area of structure  $i$  and  $n$  is the number of different structures.

TABLE I  
U-VALUES OF DIFFERENT STRUCTURES [9]

Structure	U-value (W/m <sup>2</sup> K)
Outer wall	0.21
Roof	0.15
Base floor	0.21
Window	1.40

Determining the heat capacity  $C$  of the heated mass is a more challenging task. In this paper the heat capacity is formed by a 0.08 m thick concrete slab on the floor, and a 0.012 m thick chipboard on floor, walls and ceiling. Properties of these components used in the calculation of  $C$  are presented in table II.  $C$  is calculated as

$$C = \sum_{i=1}^m c_i \rho_i V_i \quad (7)$$

where  $\rho_i$ ,  $V_i$  and  $c_i$  are density, volume and specific heat capacity of component  $i$  respectively and  $m$  is the number of components.

TABLE II  
PROPERTIES OF COMPONENTS OF EFFECTIVE HEAT CAPACITY [10]

Component	Density (kg/m <sup>3</sup> )	Specific heat capacity (J/kgK)
Concrete slab	640	2400
Chipboard	2400	840

Heating power  $P_{heat}$  is determined in accordance with a “power density” (the proportion of power to room volume) 25 W/m<sup>3</sup>.

The data presented above is used to determine thermodynamic parameters of a particular room (“prototype room”) with certain dimensions. The room is 2.5 m high, 3.5 m long and 3.5 m wide, and total area of its windows is 2 m<sup>2</sup>. Half of the room’s wall area is outer wall. Heat transfer through inner wall is assumed to be zero. Using this data, heat capacity, thermal conductance and heating power of the room are calculated and the results are presented in table III.

Using parameter values  $C$  and  $G$  of table III an example calculation of the rate of temperature decline was carried out. When the outer temperature was  $-1$  °C temperature decline from 22 °C to 20 °C took about 5 hours. The order of

magnitude of this time corresponded to the rates of temperature decline presented in [11], where cooling of a school in Finland was measured.

TABLE III  
THERMODYNAMIC PARAMETERS OF THE “PROTOTYPE ROOM”

Parameter	Value
$C$	$2.9 \cdot 10^6$ J/K
$G$	14 W/K
$P_{heat}$	770 W

In the simulations a great number of loads were added to the power system, and thermodynamic parameters had to be determined for each load. Parameters were determined randomly with MATLAB software. In the determination process the parameters of the “prototype room” were used as a reference. First, values of  $C$  were formed so that they were normally distributed having value of table III as a mean and 5% (proportion of mean value) standard deviation. After this the values of  $G$  and  $P_{heat}$  were formed so that the relative differences of different values of  $G$  and relative differences of different values of  $P_{heat}$  were equal to relative differences of different values  $C$ , regarding each load. Then random components with zero mean value and 1 % standard deviation were added to the values of  $G$  and  $P_{heat}$ . Outer temperatures of different loads were normally distributed with a  $-10$  °C mean and 1 °C standard deviation. Values of  $T_{tol}$  and  $T_{des}$  (refer to fig. 1) were uniformly distributed at intervals 0.6...1.0 °C and 19...22 °C, respectively. Initial indoor temperatures  $T_i(0)$  were uniformly distributed at interval  $T_{des} \pm 0.5T_{tol}$ . Maximum drop of temperature setting value  $\Delta T_{max}$  was set to 3 °C for each load.

#### IV. SIMULATIONS

Simulations were carried out mainly with PSCAD software. Parameters of the loads and initial values were formed with MATLAB and transferred at the first time step to PSCAD through the interface between PSCAD and MATLAB. States of frequency dependent space heating loads were not updated every time step, but every 20 ms. This was done to reduce computing time. Every time step in which operation of space heating loads were modeled, temperatures (in accordance with (5)) and on/off information of each 580,000 loads were updated. For modeling the loads, a new PSCAD component was built using Fortran programming language. PSCAD’s computing time step was 100  $\mu$ s. In this work two different cases were simulated.

##### A. Case 1: tripping of generator

In case 1, generator  $G_4$  was tripped off suddenly at 10 s with a power output of 400 MW. The length of the simulation was 900 s (15 min). Length is chosen so that it corresponds with the typical starting time of gas turbines used as disturbance or contingency reserve of a power system.

In fig. 4 frequencies which were measured from nodes 7 and 8 are presented at a time interval of 10...150 s. Simulation was carried out in two different conditions: with and without frequency dependency of the space heaters. Without frequency dependent load (fdl), the system goes into a severe instable

state, and frequency goes down near 57 Hz in 150 s leading to a total collapse of the system. With frequency dependent load, a much higher frequency level is maintained and collapse during simulation period is avoided.

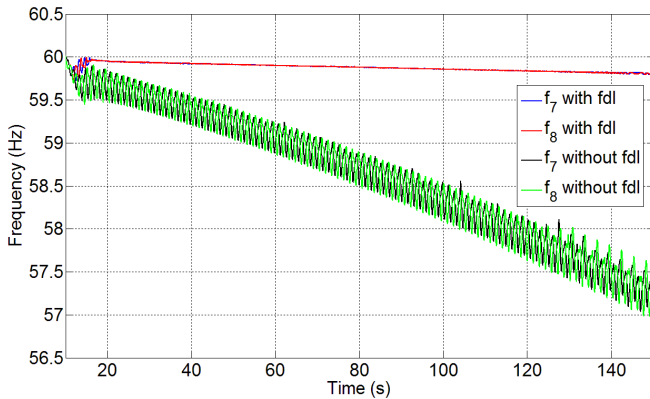


Fig. 4. Frequency behavior of the grid at time interval 10...150 s in case 1

In fig. 5, frequencies and frequency dependent loads' powers during the whole simulation period are presented. Due to frequency swing around time 12 s a great portion of the space heaters are switched off. Part of the decrease of powers during the frequency swing was due to decrease of voltages at nodes 7 and 8. Loads were modeled as constant impedance loads, and their powers are proportional to grid voltage squared. In fig. 6, frequencies, powers and voltages are presented at time interval 9.5...17 s. Voltage change from 1.02 p.u. to 0.96 p.u. corresponds with a load decrease of about 12 %, which has a significant effect on powers drawn by the space heating loads. This effect can be observed also in simulation in which frequency dependency function was not applied. It can also be observed in fig. 6 that local maximums in voltage curves often correspond with local maximums in power curves. In fig. 5, the "ripple" in frequency curve which seems to "change sign" around time 600 s is probably due to the frequency measurement method used in PSCAD software.

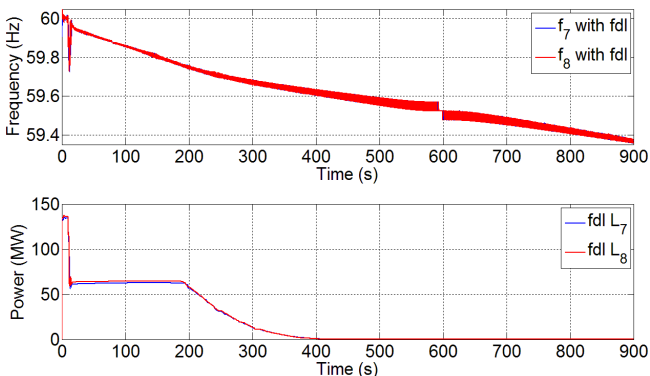


Fig. 5. Frequencies and frequency dependent loads' powers during the whole simulation period of case 1

Space heaters which switched off do not turn back on, when frequencies recover at higher levels around time interval 12...16 s. This is because the frequency rise returns only the setting values and not the original on/off states of the loads. Loads which switch off turn back on when their temperatures fall to a low enough level. After frequency swing frequencies

keep decreasing and load levels stay at a rather steady level at time interval 20...180 s, as can be seen in fig. 5. After 180 s load level continues falling in accordance with frequency fall until all space heaters are switched off.

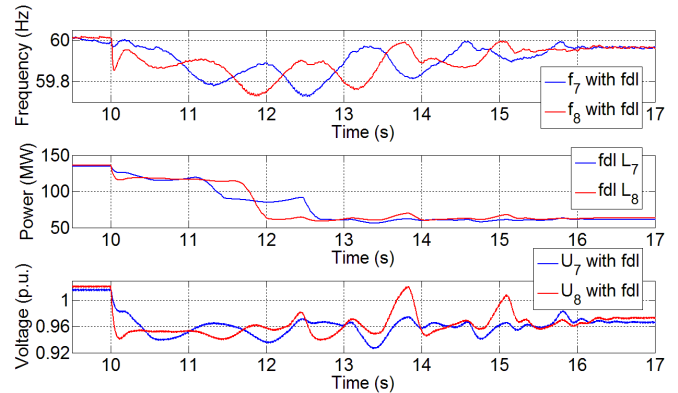


Fig. 6. Frequencies, powers and voltages at time interval 9.5...17 s in case 1

### B. Case 2: load changes

In case 2, a linearly from zero to 400 MW up ramping extra load (disturbance) was introduced in the system at node 8 at time interval 10...70 s, and load ramped down to zero at time interval 900...960 s. Length of the simulation was 10000 s, which is about 2 h 47 min.

In fig. 7 frequencies of the system are presented at time interval 0...425 s with and without frequency dependency of the loads. As in case 1, without frequency dependent load (fdl) the power system soon gets to a point of total collapse. It can be seen that without frequency dependent load frequencies fall fairly slowly after 400 MW load increase. Reason for this is a voltage drop from 1.02 p.u. to 0.96 p.u. during load increase at time interval 10...70 s, which decreased the total load remarkably. This might be too positive a result, because in reality tap changing transformers could increase the voltage at this time scale in the distribution networks, which would increase the load levels.

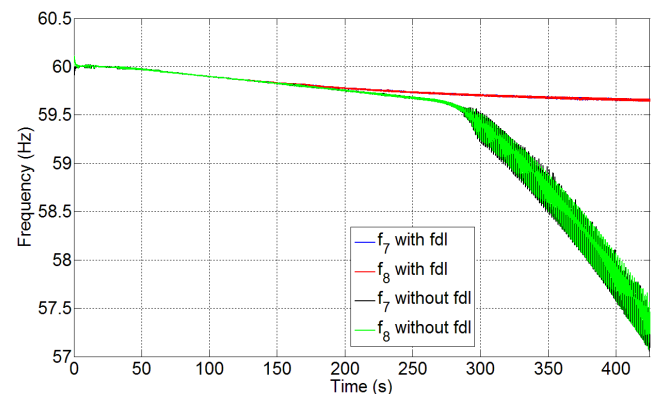


Fig. 7. Frequency behavior of the grid at time interval 0...425 s in case 2

Fig. 8 illustrates the frequencies and powers of the frequency dependent loads in case 2 during the whole simulation period. As an overview it can be said that the result is clearly better than the result without frequency dependent load. Frequencies stay at fairly high levels during the whole simulation.

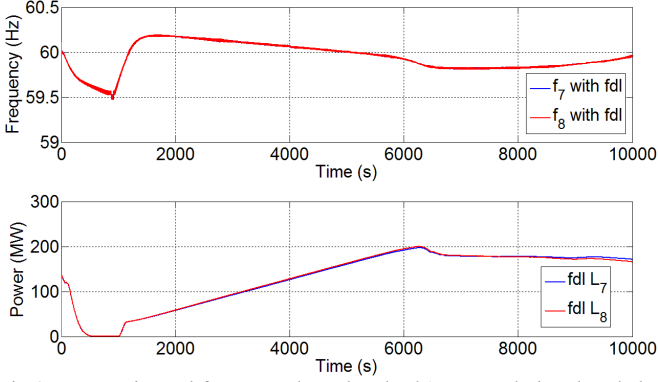


Fig 8. Frequencies and frequency dependent loads' powers during the whole simulation period of case 2

In fig. 8 an interesting phenomena can be observed. After the disturbance, powers of frequency dependent loads rise and exceed the initial values (approx. 130 MW) of the powers. In simulation of case 2, this “cold load pick-up” phenomena can be divided into two parts which can be understood more clearly by examining fig. 9.

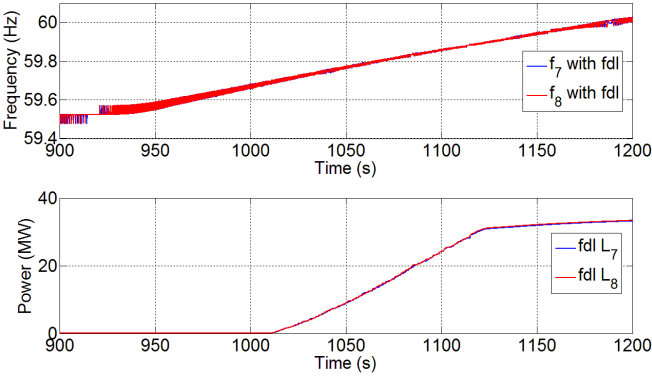


Fig. 9. Frequencies and frequency dependent loads' powers of case 2 at time interval 900...1200 s

In fig. 9, the frequencies and powers are presented at time interval 900...1200 s. When the “disturbance” load begin to ramp down, frequencies start to increase. When frequencies reach values close to 59.7 Hz, loads whose temperatures had fallen below their  $T_{des} - 0.5T_{tol}$  value (refer to fig. 1) begin to switch on in accordance with frequency rise (on-switching of individual load occurs when its on-triggering temperature, reaches the real temperature of the load) until frequencies reach a value slightly below the highest threshold frequency  $f_i$  (59.9 Hz) at time around 1125 s. After this the rate of load increase decreases. The reason is as follows. At approx. time 600 s all loads were switched off and their temperatures began to fall. After the set values of thermostats of all loads are recovered to their original values ( $T_{des}$ ) at time 1125 s, those loads that are still switched off begin to switch on gradually as their temperatures fall below the value  $T_{des} - 0.5T_{tol}$ . Because temperatures fall very slowly, the rate of load increase is also slow. When comparing temperatures at the beginning of the simulation and at time 900 s (15 min difference), the mean temperature decline was about 0.1 °C and standard deviation of temperature decline was 0.04 °C.

As can be seen in fig. 8, individual loads continue switching on until powers of  $L_7$  and  $L_8$  reach values of about 200 MW. Part of the loads is taking back the thermal energy which was dissipated during low grid frequencies. A greater number of loads are on simultaneously (trying to reach the value  $T_{des} + 0.5T_{tol}$ ) when compared to normal and steady conditions, which causes a greater total power of space heating loads. In this simulation, the power system was operating in very tight power conditions. Because of the high total power of frequency dependent loads caused by cold load pick-up phenomenon, frequencies begin to decrease again. This forces some frequency dependent loads to switch off again, and frequencies rise again to a slightly higher level. It can be thought that a down ramping disturbance load at 900...960 s could simulate a reserve capacity, which is operating as a contingency reserve. This reserve should be planned to also be able to cover the extra power caused by the cold load pick-up.

Behavior of the frequency dependent loads after the cold load pick-up could not be investigated in this simulation, because the simulation was not long enough. However, a simulation was carried out (not presented in this paper), in which the heat capacities of the loads were much smaller than in this work. Low heat capacity corresponds with a greater rate of change of temperature and faster phenomena. In the simulation, powers of the frequency dependent loads seemed to stabilize (after cold load pick-up) approximately to the levels of the initial powers of the simulation.

## V. CONCLUSIONS AND DISCUSSION

Using frequency dependent space heating load as a contingency reserve seems to be a very powerful method to manage frequency disturbances in a power system. It could be used to enhance the reserves of the power system. When using frequency dependent space heaters the effect of cold load pick-up has to be taken into account.

When using frequency dependent load in power system frequency control, it is necessary to coordinate its operation with other frequency control actions. As a result of using only space heaters as frequency dependent loads, the availability of the control resource is strongly dependent on outer temperature conditions, and at warm seasons the control resource might not be available at all. For this reason, this kind of load cannot alone substitute any spinning or contingency reserve. However, the use of space heaters could be an option for shedding of big industrial loads, which are available for controlling due to contracts between industrial companies and the grid operator. If space heating loads are not available, industrial loads are shed instead. It is less harmful to cut domestic heaters off for a while than interrupting or disturbing a whole industrial process. The availability of the space heating load can be estimated by the system operator by using load models that take weather conditions into account. If other load types, for example other heating systems, refrigerators, freezers, air conditioners, water heaters, pumps ovens [5] and in the future plug-in vehicles (plug-in hybrid electric vehicles and electric vehicles), were also used as frequency dependent loads, availability of total reserve would be much higher.

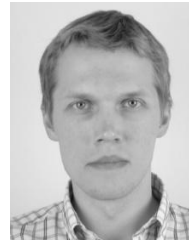
The studies presented in this paper include many simplifications and sources of error when compared to real world systems. Firstly, models used in the simulations were very simple. The power system model was a small one, and it did not include any dynamic voltage regulation equipment besides generator exciters. Protection equipment of generators were not modeled and loads were modeled simply by constant impedance loads. Modeling frequency dependent loads in a transmission network level also brings a somewhat of an error source, because small dynamic phenomena between transmission network and low voltage network is excluded from the simulations except the small delay added to the frequency measurement filter presented in (1). The thermodynamic model did not include the effect of ventilation. In addition to heaters, other electrical loads and humans inside the buildings also produce heat. However, the effects of ventilation and other heat sources besides heaters partly compensate each other. Thermodynamic parameters of different loads were distributed hypothetically, and distributions were not based to any particular stock of buildings.

Future work in this field is needed. Longer simulations with more sophisticated and accurate models should be carried out, and also different kinds of practical demonstrations should be built. The authors of this paper are working on a practical demonstration, in which a single frequency dependent space heating load which exploits a commercial smart meter is demonstrated in a laboratory environment. It is also very important to investigate different regulatory and market related issues regarding to the use of this load control method. The authors are also researching the use of frequency dependent charging of plug-in vehicles to enhance the frequency stability of power systems.

## VI. REFERENCES

- [1] UCTE, "Final report of the Investigation Committee on the 28 September 2003 Blackout in Italy", [Online] Available: [http://www.ucte.org/\\_library/otherreports/20040427\\_UCTE\\_IC\\_Final\\_report.pdf](http://www.ucte.org/_library/otherreports/20040427_UCTE_IC_Final_report.pdf)
- [2] UCTE, "Final Report, System Disturbance on 4 November 2006, union for the co-ordination of transmission of electricity", [Online] Available: [http://www.ucte.org/\\_library/otherreports/Final-Report-20070130.pdf](http://www.ucte.org/_library/otherreports/Final-Report-20070130.pdf)
- [3] U.S.-Canada Power System Outage Task Force, "Final Report on the August 14, 2003 Blackout in the United States and Canada: Causes and Recommendations", [Online] Available: <https://reports.energy.gov/BlackoutFinal-Web.pdf>
- [4] F. C. Schweppe, "Frequency adaptive, power-energy re-scheduler", U.S. Patent 4317049
- [5] J. A. Short, D. G. Infield and L. L. Freris, "Stabilization of Grid Frequency through Dynamic Demand Control", IEEE Transactions on Power Systems, vol. 22, 3, pp. 1284–1293, 2007
- [6] P. Kundur, "Power System Stability and Control", McGraw-Hill, Inc., 1994, 979 p.
- [7] Klein, M., Rogers, G. J., Kundur, P., "A fundamental study of inter-area oscillations in power systems", IEEE Transactions on Power Systems, vol. 6, 3, pp. 914-921, 1991
- [8] J. Chow/Cherry Tree Scientific Software, "Power System Toolbox, Version 2.0, Dynamic Tutorial and Functions", 171 p.
- [9] Finland's environmental administration, "Heat insulation of buildings", Regulations 2007, C3 Collection of Finnish building regulations, 9 p. (In Finnish)
- [10] T. Kalema, "Heating and Ventilating Engineering, part 2", Tampere University of Technology, Department of Energy and Process Engineering, 195 p. (In Finnish)
- [11] R. Kohonen, "Discontinuous heating of buildings", National technical research center, Researches 152, Espoo, 1983 (In Finnish)

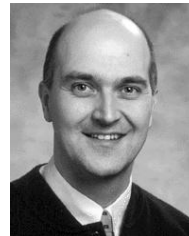
## VII. BIOGRAPHIES



**A. Rautiainen** received his M.Sc degree from Tampere University of Technology in 2008. He is now working as a researcher towards doctoral degree at Tampere University of Technology. His main interest focuses on the using of frequency dependent load to improve power system's frequency stability and effects of plug-in vehicles to electric power systems.



**S. Repo** received his M.Sc. and Dr.Tech. degrees in Electrical Engineering from Tampere University of Technology in 1996 and 2001 respectively. At the present he is a University Lecturer at the Department of Electrical Energy Engineering of Tampere University of Technology. His main interest is the management of active distribution network including distributed energy resources.



**P. Järventausta** received his M.Sc. and Licentiate of Technology degrees in Electrical Engineering from Tampere University of Technology in 1990 and 1992 respectively. He received the Dr.Tech. degree in Electrical Engineering from Lappeenranta University of Technology in 1995. At present he is a professor at the Department of Electrical Energy Engineering of Tampere University of Technology. The main interest focuses on the electricity distribution and electricity market.